EAI Endorsed Transactions
on Scalable Information Systems

Research Article EAI.EU

A New Waveform Design for Wireless Communication: High-Rate DCSK Scheme with Joint Three-dimensional Index Modulation

Chao Duan[1], Panpan Yin[1,*]

[1]School of Integrated Circuits and New Enegy, Guangzhou College of Technology and Business, Foshan, 528138, China

Abstract

INTRODUCTION: This paper develops a differential chaos shift keying scheme with joint three-dimensional index modulation, termed the JTIM-DCSK scheme.
OBJECTIVES: To achieve higher transmission efficiency and enhanced bit-error-ratio (BER) performance through advanced waveform design.
METHODS: In the proposed scheme, to improve spectrum utilization and increase waveform flexibility, a Hilbert transform–based processing structure is introduced, enabling information bits to be mapped onto time slots and subcarriers that would otherwise remain unused. Furthermore, the overall transmission efficiency of the proposed JTIM-DCSK scheme is substantially enhanced by incorporating code-index modulation into the reference chaotic waveform. To further improve the BER performance and strengthen the robustness against noise and channel fading, a conventional noise reduction algorithm is employed at the receiver.
RESULTS: Comparative evaluations in terms of data rate, computational complexity, and BER performance demonstrate the clear superiority of the proposed scheme over existing counterparts.
CONCLUSION: Therefore, the JTIM-DCSK scheme represents a promising waveform design candidate for secure short-range wireless communications in multi-path Rayleigh fading channels.

Keywords: Chaotic waveform, indexed modulation, channel fading, noise-reduction, data rate

Received on 17 July 2026, accepted on 03 November 2026, published on 27 November 2026

Copyright © 2026 Chao Duan *et al.*, licensed to EAI. This is an open access article distributed under the terms of the CC BY-NC-SA 4.0, which permits copying, redistributing, remixing, transformation, and building upon the material in any medium so long as the original work is properly cited.

doi: 10.4108/eetsis.16551

1. Introduction

Chaotic waveforms have recently attracted considerable attention in the context of modern communication system designs[1]. This growing interest stems from their inherent resistance to fading, low power consumption, and favorable security properties, which make them particularly suitable for multi-path Rayleigh fading channels [1, 2]. In general, chaotic modulation techniques can be categorized into two primary types, namely coherent schemes and incoherent schemes [3]. Within this framework, the differential chaos shift keying (DCSK) system has received increasing research focus due to its strong robustness, enhanced security characteristics, and its capability to support flexible waveform configurations in harsh wireless environments[4–6].

Conventional DCSK schemes suffer from low spectral and energy efficiency because one half of each transmission frame must be allocated to transmitting reference signals. In addition, the receiver structure generally relies on radio-frequency (RF) delay lines, whose practical implementation remains challenging with existing hardware technologies. To address these fundamental drawbacks of traditional DCSK architectures, a variety of enhanced DCSK variants have been proposed in the literature [7–10], thereby driving chaotic communication research into a new stage of development. In an

*Corresponding author. Email: panpanyin@gzgs.edu.cn

effort to remove the dependence on RF delay lines, the code-shifted DCSK (CS-DCSK) scheme was introduced in [11, 12]. Building upon this line of research, a high-efficiency DCSK (HE-DCSK) approach was later reported in [13], where each reference sample is reutilized twice during modulation, thereby increasing the achievable throughput. To further improve transmission efficiency, the short-reference DCSK (SR-DCSK) scheme proposed in [14] reduces the length of the reference segment, enabling higher data rates. Meanwhile, the multi-carrier DCSK (MC-DCSK) schemes in [15–18] adopts a parallel multi-carrier architecture that avoids RF delay components and facilitates high-speed data transmission. In [19], a differential DCSK (DDCSK) scheme was developed, exhibiting strong resistance to inter-symbol interference (ISI) and favorable performance in multi-user scenarios. Moreover, the trinal-code-shift DCSK (TCS-DCSK) scheme presented in [20] effectively addresses the difficulty of utilizing reference signals for information transmission in conventional DCSK systems. More recently, the incorporation of index modulation into DCSK frameworks has become a major research direction [21–23]. By mapping additional information bits onto extra transmission resources, these schemes markedly improve spectral efficiency and overall throughput. To support high-data-rate applications, a multidimensional-index-modulated DCSK (MIM-DCSK) scheme was proposed in [24–27]. In addition, the hybrid-index-modulated multi-carrier DCSK (HIM-MC-DCSK) schemes in [28–30] integrate both carrier index and carrier-number index modulation within a multi-carrier structure, achieving significant enhancements in both energy and spectrum utilization. Nevertheless, despite these notable improvements, many index-assisted DCSK designs entail increased structural complexity. Therefore, developing a simplified modulation architecture that preserves excellent bit error rate (BER) performance continues to be an important and unresolved research issue.

Based on the motivation of satisfying the ever-increasing requirements for high-data-rate wireless transmission, a joint three-dimensional index modulation-based DCSK scheme, referred to as the JTIM-DCSK scheme, is developed by embedding three-dimensional indexing resources into the conventional DCSK architecture, thereby constructing a more adaptable and efficient chaotic waveform framework. Within this scheme, information bits are conveyed by jointly utilizing subcarriers and time slots through the Hilbert transform, which enhances both resource utilization efficiency and waveform design flexibility. In addition, the code index bits are demodulated separately from the other index components, so that their detection process does not affect the recovery of the remaining index bits. Consequently, the proposed JTIM-DCSK system is well suited to support multi-path Rayleigh fading channel scenarios. To further enhance transmission reliability and resilience to channel impairments, a noise mitigation strategy is incorporated at the receiver to alleviate interference effects. Comprehensive evaluations in terms of achievable data rate, computational complexity, and BER performance confirm that the proposed scheme outperforms existing advanced DCSK-based approaches, demonstrating its promise as a robust and high-efficiency waveform solution for future wireless communication systems.

The main contributions of this paper are summarized as follows.

1. A joint three-dimensional index modulation framework is developed for DCSK schemes, which improves spectral efficiency and waveform flexibility by jointly exploiting subcarriers and time slots through the Hilbert transform.

2. An independent demodulation mechanism for code index bits is designed, preventing mutual interference among different index components while maintaining low complexity.

3. A receiver-side noise mitigation strategy is incorporated to enhance robustness against channel impairments, and comprehensive evaluations verify that the proposed scheme achieves improved data rate and BER performance compared with existing DCSK-based schemes.

The remainder of this paper is organized as follows. Section 2 presents the system model of the proposed JTIM-DCSK scheme. Section 3 elaborates on the complexity and efficiency analysis of the proposed JTIM-DCSK scheme. Section 4 shows simulation results and Section 5 concludes the paper.

2. System model

2.1. Transmitter

2.1.1. Chaotic Generator

The chaotic generator utilizes a second-order Chebyshev polynomial function[3, 5] defined as $x_{k+1} = 1 - 2x_k^2$, to produce a reference chaotic signal $c_x = [c_{x,1}, c_{x,2}, \cdots, c_{x,\theta}]$, where $k = 1, 2, \ldots, \theta$, and θ represents the length of the reference chaotic signal. Additionally, an orthogonal chaotic signal $c_y = [c_{y,1}, c_{y,2}, \cdots, c_{y,\theta}]$ corresponding to c_x can be generated by applying a Hilbert transform, fulfilling the condition $\sum_{k=1}^{\theta} c_{x,k} c_{y,k} = 0$.

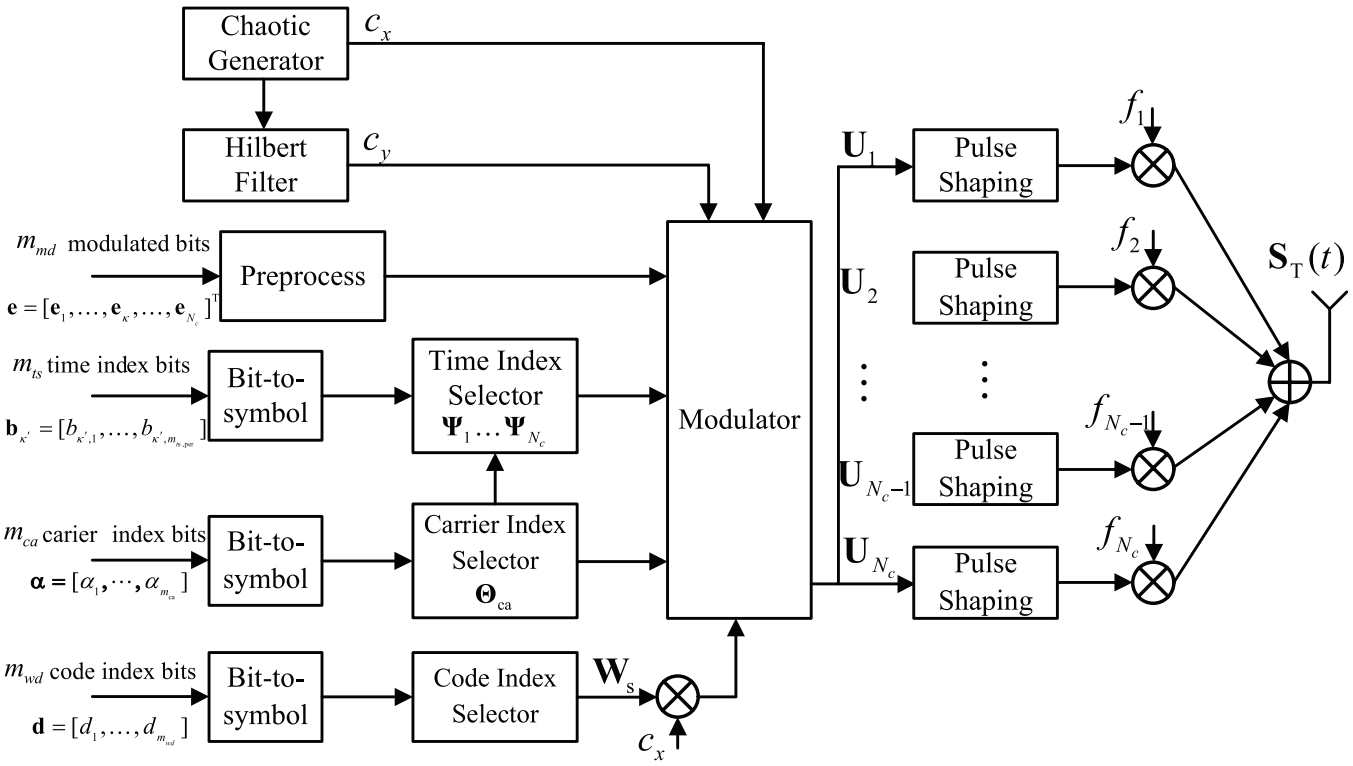

Figure 1. Transmitter structure of the proposed JTIM-DCSK system

2.1.2. Index selector

Fig. 1 illustrates the transmitter architecture of the proposed JTIM-DCSK system. In this scheme, the total number of subcarriers is denoted as N_c, where each subcarrier occupies N_t+1 time slots. The 0-th time slot is dedicated to transmit the reference chaotic signal. Among these subcarriers, N_c-1 are selected to convey $m_{ca}=\log_2(N_c)$ bits via carrier index modulation. For every selected subcarrier, N_t-1 out of N_t time slots are selected to convey $m_{ts,per}=\log_2 N_t$ time slot index bits, so that $m_{ts}=(N_c-1)m_{ts,per}$ time index bits are transmitted in each JTIM-DCSK symbol period. Additionally, only the first subcarrier's reference chaotic signal is employed for code index modulation using N_{wd}-order Walsh code. The number of code index bits is $m_{wd}=\log_2 N_{wd}$. Beyond these three forms of index bits, the scheme also integrates a DCSK modulation scheme to transmit $m_{md}=N_c\cdot N_t$ modulated bits. Specifically, the unselected subcarriers and time slots are designed to transmit the modulated bits through c_y, and the remaining selected subcarriers and time slots are designed to carry the modulated bits through c_x . Hence, the total number of transmitted bits per JTIM-DCSK symbol duration is given by $m_{tot}=m_{ca}+m_{ts}+m_{wd}+m_{md}$.

The carrier index bits $\alpha=[\alpha_1,\cdots,\alpha_{m_{ca}}]$ generate the corresponding carrier index mapping symbol r through carrying out bit/symbol conversion and the carrier index mapping symbol r represents that the r-th subcarrier is unselected, and then the carrier index vector is assumed to be defined a s $\mathbf{\Theta}_{ca}=[\Theta_{ca,1},\cdots,\Theta_{ca,\kappa},\cdots,\Theta_{ca,N_c}]$, where $\Theta_{ca,\kappa}\in\{0,1\}$, $\Theta_{ca,\kappa}=0$ represents that the κ-th subcarrier is unselected and $\Theta_{ca,\kappa}=1$ represents that the κ-th subcarrier is selected. This is called carrier index modulation. Assuming that the time index vector is $\mathbf{\Psi}=[\mathbf{\Psi}_1,\cdots\mathbf{\Psi}_\kappa,\cdots,\mathbf{\Psi}_{N_c}]^T$, where $\mathbf{\Psi}_\kappa=[\Psi_{\kappa,0},\ldots,\Psi_{\kappa,\chi},\ldots,\Psi_{\kappa,N_t}]$ denotes the time index vector in the κ-th subcarrier, $1\le\kappa\le N_c$, $0\le\chi\le N_t$, and "T" denotes the transpose operation. In the time index vector $\mathbf{\Psi}$, since the r-th subcarrier is not selected, $\Psi_r=[1\ \mathrm{O}_{1\times N_c}]$, where $\mathrm{O}_{1\times N_c}$ denotes a $1\times N_c$ zero matrix. Because the 0-th time slot is allocated to the reference chaotic signal, $\Psi_{\kappa,0}=1$. Moreover, $\Psi_{\kappa,\chi}=1$ and $\Psi_{\kappa,\chi}=0$ indicate that the χ-th time slot is selected and unselected in the κ-th subcarrier, respectively. In the selected subcarrier, only one $\Psi_{\kappa,\chi}=0$, and the rest of the elements are all 1.

The unselected time slot in the κ'-th selected subcarrier is defined by the κ'-th time indexed symbol $v_{\kappa'}$, it is the result of the transformation of bit/symbol conversion on the time index bits $\mathbf{b}_{\kappa'}=[b_{\kappa',1},\ldots,b_{\kappa',m_{ts,per}}]$. This is called time slot index modulation. The computational relationship between κ

and κ' is represented as

$$\kappa' = \begin{cases} \kappa & \kappa \le r, \\ \kappa - 1 & \kappa > r. \end{cases} \tag{1}$$

In the JTIM-DCSK system, the 0-th time slot of the first subcarrier is designed to transmit the code index symbol s by selecting s-th row of the Walsh code matrix, i.e., $W_{N_{wd},s} = [w_{N_{wd},s,1}, \ldots, w_{N_{wd},s,i}, \ldots, w_{N_{wd},s,N_{wd}}]$, which is referred to as code index modulation. In particular, the code index symbol s is derived by converting the code index bits $\mathbf{d} = [d_1, \ldots, d_{m_{wd}}]$ through a bit-to-symbol transformation, $w_{N_{wd},s,i}$ represents an element in a Walsh code of length N_{wd} . Since there is a reference chaotic signal that will perform code index modulation, the signal in the 0-th time slot of the κ-th subcarrier in the JTIM-DCSK system is represented by

$$G_\kappa = \begin{cases} c_x & \kappa \ne 1, \\ [w_{N_{wd},s,1}\hat{c}_{x,1}, \ldots, w_{N_{wd},s,i}\hat{c}_{x,\chi}, & \\ \ldots, w_{N_{wd},s,N_{wd}}\hat{c}_{x,N_{wd}}] & \kappa = 1, \end{cases} \tag{2}$$

where c_x denotes a chaotic signal of length θ, and $\hat{c}_{x,i}$ can be expressed by the formula

$$\hat{c}_{x,i} = \left[c_{x,(i-1)\frac{\theta}{N_{wd}}+1}, \ldots, c_{x,i\frac{\theta}{N_{wd}}} \right]. \tag{3}$$

The modulated bits are denoted as $\mathbf{e} = [e_1, \ldots, e_\kappa, \ldots, e_{N_c}]^T$, where $\mathbf{e}_\kappa = [e_1, \ldots, e_\chi, \ldots, e_{N_t}]$, $e_{\kappa,\chi} \in \{0, 1\}$. The modulated bits are preprocessed to perform the polarity conversion, which is represented as

$$g_{\kappa,\chi} = \begin{cases} 1 & e_{\kappa,\chi} = 1, \\ -1 & e_{\kappa,\chi} = 0. \end{cases} \tag{4}$$

Therefore, the signal of the κ-th subcarrier is represented as

$$\mathbf{U}_\kappa = [G_\kappa, u_\kappa(1), u_\kappa(2), \ldots, u_\kappa(\chi), \ldots, u_\kappa(N_t)], \tag{5}$$

$$u_\kappa(\chi) = \begin{cases} g_{\kappa,\chi}c_x & \Psi_{\kappa,\chi} = 1, \\ g_{\kappa,\chi}c_y & \Psi_{\kappa,\chi} = 0, \end{cases} \tag{6}$$

where $\Psi_{\kappa,\chi} = 1$ and $\Psi_{\kappa,\chi} = 0$ indicate that the χ-th time slot is selected and unselected in the κ-th subcarrier, respectively. The overall transmitted signals of the JTIM-DCSK system are depicted as follows

$$\mathbf{S} = [\mathbf{U}_1, \ldots, \mathbf{U}_\kappa, \ldots, \mathbf{U}_{N_c}]^T, \tag{7}$$

where $\mathbf{U}_\kappa = [G_\kappa, u_\kappa(1), u_\kappa(2), \ldots, u_\kappa(\chi), \ldots, u_\kappa(N_t)]$, $1 \le \kappa \le N_c$ and "T" denotes the transpose operation.

Fig. 2 illustrates an sample of signal format of the proposed JTIM-DCSK system, where $N_c = 4$, $N_t = 4$, $N_{wd} = 4$, $G(W_{N_{wd},s}, c_x)$ denotes the code index modulation

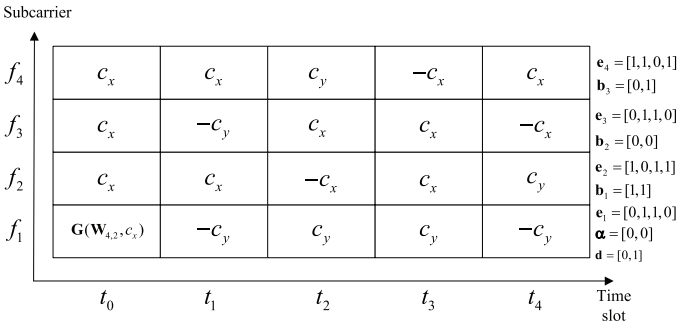

Figure 2. An example of signal format for the JTIM-DCSK system

modulation

$$G(W_{N_{wd},s}, c_x) = [w_{N_{wd},s,1}\hat{c}_{x,1}, \ldots, w_{N_{wd},s,i}\hat{c}_{x,\chi}, \ldots, w_{N_{wd},s,N_{wd}}\hat{c}_{x,N_{wd}}], \tag{8}$$

$\mathbf{d} = [0, 1]$ is the code index bit, and it selects 2-th row of the Walsh code matrix. $\alpha = [0, 0]$ is the carrier index bit, it indicates that the first subcarrier is not selected. $\mathbf{b}$ is the time slot index bit, $b_1 = [1, 1]$ denotes that the 4-th time slot of the 2-th subcarrier is unselected. The unselected subcarriers and time slots are designed to transmit the modulated bits through c_y, and the remaining selected subcarriers and time slots are designed to carry the modulated bits through c_x .

2.1.3. Transmission process

Afterwards, the signals $\mathbf{U}_\kappa$ $(1 \le \kappa \le N_c)$ are passed through the pulse shaping filter $h_l(t)$. Following this process, the corresponding synthesized signals are derived as follows:

$$s_\kappa(t) = \sum_{i=1}^{(N_t+1)\theta} U_{\kappa,i} h_l(t - iT_c), \tag{9}$$

where T_c denotes the chip duration. And the synthesized signals are then transmitted by the corresponding subcarriers. Thus, the obtained transmitted signals are represented as

$$s_T(t) = \sum_{\kappa=1}^{N_c} s_\kappa(t) \cos(2\pi f_\kappa t + \phi_\kappa), \tag{10}$$

where ϕ_κ denotes the phase angle, $U_{\kappa,i}$ denotes the element of the transmitted signals of the κ-th subcarrier. In addition, the spreading factor of the JTIM-DCSK system is represented as $\beta = (N_t + 1)\theta$.

2.2. Receiver

2.2.1. Channel model

This paper examines an L-path Rayleigh fading channel characterized by the channel coefficient λ_l and time

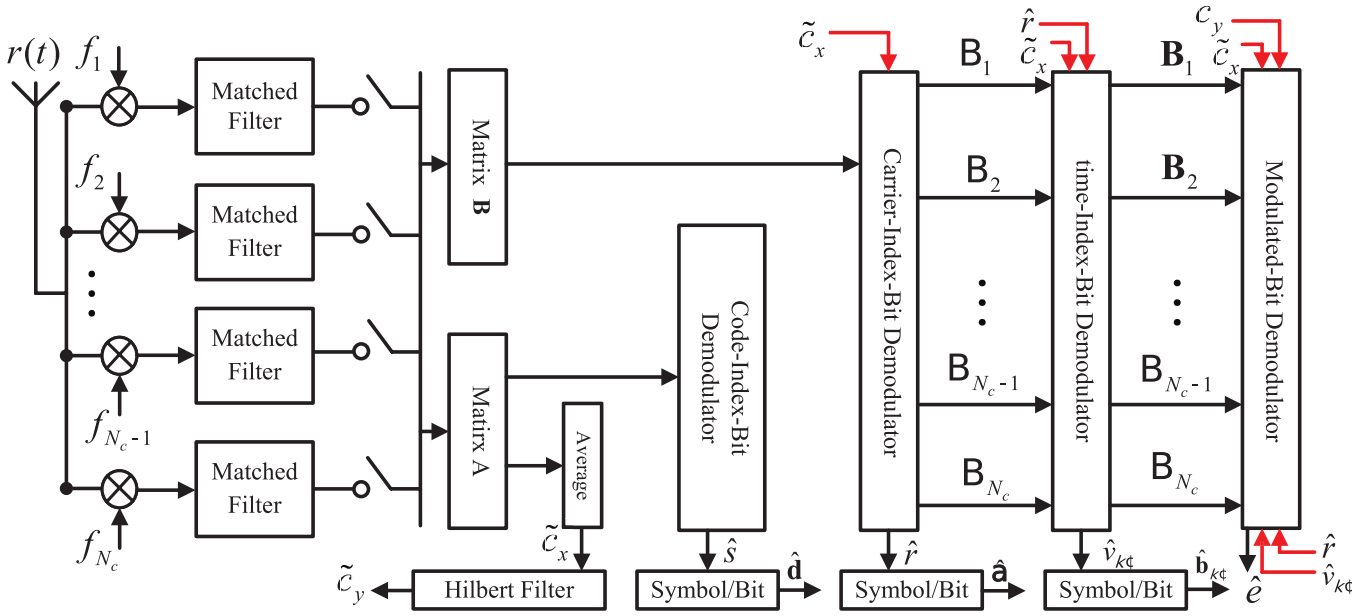

Figure 3. Receiver structure of the proposed JTIM-DCSK system

delay τ_l, as follows[9, 11]:

$$h(t) = \sum_{l=1}^{L} \lambda_l \delta(t - \tau_l). \tag{11}$$

2.2.2. Receiving process

The structure of the JTIM-DCSK receiver is illustrated in Fig. 3. During transmission over a Rayleigh fading channel, the signals are subjected to additive white Gaussian noise, and the received signal is denoted as

$$r(t) = s_T(t) * h(t) + n(t), \tag{12}$$

It is assumed that the maximum multipath delay is considerably shorter than the spreading factor, thereby allowing inter-symbol interference (ISI) to be neglected. Furthermore, perfect carrier synchronization is presumed at the receiver side, effectively eliminating inter-carrier interference (ICI).

The received signals are first separated by their corresponding orthogonal carriers, followed by matched filtering operations tailored to each carrier. After demodulation, the resulting signals are categorized into two types: information-bearing signals and reference signals. Specifically, N_c reference signals are stored into matrix $\mathbf{A}$ with dimension of $N_c \times \theta$, while N_c information-bearing signals are stored in matrix $\mathbf{B} = \{B_{i,j}\} = [\mathbf{B}_1, \ldots, \mathbf{B}_{N_c}]^T$, where $1 \le i \le N_c$ and $1 \le j \le (N_t + 1)\theta$. To enhance the BER performance, the influence of Gaussian noise on the reference signals can be mitigated through various noise reduction techniques. In particular, the received reference signals are summed and averaged, and the average reference signal obtained after the noise reduction algorithm can be expressed as

$$\tilde{c}_x = \frac{1}{N_c - 1} \sum_{u=2}^{N_c} \sum_{k=1}^{\theta} \left(\sum_{l=1}^{L} \lambda_l c_{x,k-\tau_l} + n_{x,k}^u \right). \tag{13}$$

1) Detection of Code-Index-Bits: This modulation is performed only on the reference signal of the first subcarrier. First, $\tilde{c}_x$ is computed with the N_{wd}-order Walsh code to obtain N_{wd} copies, and the o-th copy can be expressed as

$$D_o = G(W_{N_{wd},o}, \tilde{c}_x) = [D_{o,1}, \ldots, D_{o,k}, \ldots, D_{o,\theta}], \tag{14}$$

Therefore, the decision variable for code index demodulation can be expressed as

$$I_{wd,o} = \sum_{k=1}^{\theta} D_{o,k} A_{1,k}, \tag{15}$$

where $A_{1,k}$ denotes the element of the reference signal in the first subcarrier. Demodulating the code index symbol $\hat{s}$ is expressed in the following way

$$\hat{s} = \arg\max\left(I_{wd,o}\right), o = 1, \ldots, N_{wd}. \tag{16}$$

2) Detection of Carrier-Index-Bits: For the sake of demodulating the corresponding carrier-index-bits, it is necessary to use $\tilde{c}_x$ to perform a correlation operation with the information-bearing-signals of the N_t remaining time slots in each subcarrier, thus obtaining N_t correlation measures in each subcarrier,

and the χ-th correlation measure in the κ-th subcarrier can be represented by

$$I_{\kappa,\chi} = \sum_{k=1}^{\theta} \tilde{c}_{x,k} B_{\kappa,(\chi-1)\theta+k}. \tag{17}$$

More specifically, when $\kappa \neq r$ and $\chi \neq v_{\kappa'}$, it is equivalent to $\tilde{c}_x$ correlate with the information-bearing signal containing the reference signal c_x, which can be represented by

$$I'_{\kappa,\chi} = \sum_{k=1}^{\theta} \left(\sum_{l=1}^{L} \lambda_l \tilde{c}_{x,k} + \tilde{n}_{x,k} \right) \times \left(\sum_{l=1}^{L} \lambda_l e_{\kappa,\chi} c_{x,\kappa,\chi\theta+k} + n_{\kappa,\chi\theta+k} \right). \tag{18}$$

When $\kappa \neq r$ and $\chi = v_{\kappa'}$, it is equivalent to $\tilde{c}_x$ correlate with the information-bearing signal containing the orthogonal signal c_y of reference signal, which is represented by

$$I''_{\kappa,\chi} = \sum_{k=1}^{\theta} \left(\sum_{l=1}^{L} \lambda_l \tilde{c}_{x,k} + \tilde{n}_{x,k} \right) \times \left(\sum_{l=1}^{L} \lambda_l e_{\kappa,\chi} c_{y,\kappa,\chi\theta+k} + n_{\kappa,\chi\theta+k} \right). \tag{19}$$

Similarly, when $\kappa = r$, the correlation measure of the κ-th subcarrier is represented by

$$I'''_{\kappa,\chi} = \sum_{k=1}^{\theta} \left(\sum_{l=1}^{L} \lambda_l \tilde{c}_{x,k} + \tilde{n}_{x,k} \right) \times \left(\sum_{l=1}^{L} \lambda_l e_{\kappa,\chi} c_{y,\kappa,\chi\theta+k} + n_{\kappa,\chi\theta+k} \right). \tag{20}$$

For the purpose of recovering the carrier-index-bits, the absolute values of the N_t correlation measures in the κ-th subcarrier need to be computed, and then these absolute values are summed up to obtain the decision variable of the κ-th subcarrier. As a result, when $\kappa \neq r$, the decision variable of the κ-th subcarrier (selected subcarrier) is represented by

$$I_{ca,\kappa} = \left| I''_{\kappa,\chi} \right| + \left(\sum_{\chi=1,\chi\neq v_{\kappa'}}^{N_t} \left| I'_{\kappa,\chi} \right| \right). \tag{21}$$

And when $\kappa = r$, the decision variable for the κ-th subcarrier (the unselected subcarrier) are represented by

$$I'_{ca,\kappa} = \sum_{\chi=1,}^{N_t} \left| I'''_{\kappa,\chi} \right|. \tag{22}$$

The carrier index symbol r is extracted by utilizing the location of the minimum value in the decision variables $I_{ca,\kappa}$ and $I'_{ca,\kappa}$. In mathematical terms, it is as follows

$$\hat{r} = \arg\min(I_{ca,\kappa}, I'_{ca,\kappa}), \kappa = 1, \ldots, N_c. \tag{23}$$

3) Detection of Time-Index-Bits: In the JTIM-DCSK system, except for the unselected subcarrier (i.e., the $\hat{r}$-th subcarrier) in which no time index modulation is performed, it is performed in the remaining subcarriers. So as to demodulate the corresponding time-index-bits, it is necessary to use $\tilde{c}_x$ to perform a correlation operation with the signals from the other N_t time slots in each selected subcarrier, thus obtaining N_t correlation measures in each subcarrier. When $\chi \neq v_{\kappa'}$, the correlation measure for the κ'-th selected subcarrier is written as

$$I_{ts,\kappa',\chi} = \sum_{k=1}^{\theta} \left(\sum_{l=1}^{L} \lambda_l \tilde{c}_{x,k} + \tilde{n}_{x,k} \right) \times \left(\sum_{l=1}^{L} \lambda_l e_{\kappa,\chi} c_{x,\kappa,\chi\theta+k} + n_{\kappa,\chi\theta+k} \right). \tag{24}$$

And when $\chi = v_{\kappa'}$, the correlation measure for the κ'-th selected subcarrier is represented by

$$I'_{ts,\kappa',\chi} = \sum_{k=1}^{\theta} \left(\sum_{l=1}^{L} \lambda_l \tilde{c}_{x,k} + \tilde{n}_{x,k} \right) \times \left(\sum_{l=1}^{L} \lambda_l e_{\kappa,\chi} c_{y,\kappa,\chi\theta+k} + n_{\kappa,\chi\theta+k} \right). \tag{25}$$

The relationship between κ and κ' is represented by

$$\kappa' = \begin{cases} \kappa & \kappa \leq \hat{r}, \\ \kappa - 1 & \kappa > \hat{r}. \end{cases} \tag{26}$$

For the sake of recovering the time indexed symbol transmitted in the κ'-th selected subcarrier, it is necessary to identify the location of the minimum value among the correlation measures $I_{ts,\kappa',\chi}$ and $I'_{ts,\kappa',\chi}$, which can be given by

$$\hat{v}_{\kappa'} = \arg\min(I_{ts,\kappa',\chi}, I'_{ts,\kappa',\chi}), \chi = 1, \ldots, N_t. \tag{27}$$

Thus, by converting $\hat{v}_{\kappa'} - 1$ from decimal to binary, it is possible to obtain the time-index-bits.

4) Detection of Modulated-Bits: Since those bits are transmitted in the remaining N_t time slots of each subcarrier, the detection in these time slots is required. When $\kappa \neq r$ and $\chi \neq v_{\kappa'}$, the decision variable for the χ-th time slot of the κ-th selected subcarrier can be given

by

$$V_{\kappa,\chi} = \sum_{k=1}^{\theta}\left(\sum_{l=1}^{L}\lambda_l \tilde{c}_{x,k} + \tilde{n}_{x,k}\right) \times \left(\sum_{l=1}^{L}\lambda_l e_{\kappa,\chi} c_{x,\kappa,\chi\theta+k} + n_{\kappa,\chi\theta+k}\right). \quad (28)$$

otherwise ($\kappa = r$, or $\chi \neq v_{\kappa'}$), $V_{\kappa,\chi}$ is expressed as

$$V_{\kappa,\chi} = \sum_{k=1}^{\theta}\left(\sum_{l=1}^{L}\lambda_l \tilde{c}_{y,k} + \tilde{n}_{x,k}\right) \times \left(\sum_{l=1}^{L}\lambda_l e_{\kappa,\chi} c_{y,\kappa,\chi\theta+k} + n_{\kappa,\chi\theta+k}\right). \quad (29)$$

The modulated-bits are written as

$$\hat{e}_{\kappa,\chi} = \begin{cases} 1 & V_{\kappa,\chi} \geq 0, \\ 0 & V_{\kappa,\chi} < 0. \end{cases} \quad (30)$$

3. Analysis of complexity and efficiency

In this section, we evaluate the JTIM-DCSK scheme concerning data rate and complexity. Additionally, we compare the proposed JTIM-DCSK scheme with other advanced counterparts.

3.1. Analysis of data rate

Generally, the data rate refers to the number of bits transmitted per second. In the proposed JTIM-DCSK scheme, information bits are conveyed by exploiting the indices from three distinct domains. Specifically, the number of index bits is denoted as $\log_2 N_c + (N_c - 1)\log_2 N_t + \log_2 N_{wd}$, while the number of modulated bits is represented as $N_c N_t$. Therefore, the total number of transmitted bits can be expressed as $N_c N_t + \log_2 N_c + (N_c - 1)\log_2 N_t + \log_2 N_{wd}$. The transmission duration for each JTIM-DCSK scheme is βT_c . Therefore, the data rate of JTIM-DCSK system is written as

$$\xi_1 = \frac{N_c N_t + \log_2 N_c + (N_c - 1)\log_2 N_t + \log_2 N_{wd}}{\beta T_c}. \quad (31)$$

The data rates of several advanced reference schemes are summarized in Table 1, where M represents the modulation order. For a more detailed comparison, an illustrative example is provided to evaluate the data rate differences between the proposed JTIM-DCSK system and four other existing DCSK-based systems. The comparison parameters for those systems are set as follows: 1)$N_c = 4$, $N_t = 4$, N_{wd}=2 for JTIM-DCSK; 2)$N_c = 4$, $N_t = 4$, N_{wd}=2 for MIM-DCSK; 3)$N_c = 4$ for HIM-MC-DCSK, 4)$N_c = 4$, $M = 4$, N_{wd}=2 for CIM-MC-MDCSK [31]. So that the data rates for the JTIM-DCSK, MIM-DCSK [26], HIM-MC-DCSK [29], CIM-MC-MDCSK, and traditional DCSK schemes are $\frac{25}{\beta T_c}$, $\frac{16}{\beta T_c}$, $\frac{8}{\beta T_c}$, $\frac{9}{\beta T_c}$, $\frac{1}{\beta T_c}$, respectively, where the spreading factor of these five systems are kept constant. It can be observed that the proposed JTIM-DCSK system attains a higher data rate than the four compared DCSK schemes under the given scenario.

3.2. Analysis of complexity

The overall system complexity primarily comprises two components: the complexity associated with spreading/despreading operations and and the complexity of index searching. Specifically, the index searching complexity refers to the number of comparisons required to determine the unselected subcarriers, unselected time slots, and the selected Walsh code. In the proposed JTIM-DCSK scheme, N reference signals and their corresponding orthogonal versions must be generated at the transmitter. So that the complexity of spreading operation is $N_c N_t \theta + (N_c + 1)\theta$. At the receiver, the orthogonal version of the reference chaotic signal affected by the noise is obtained by the Hilbert transform, while the $N_{wd}\theta$ despreading operations are needed to demodulate the Walsh code. Additionally, the complexity of index searching is $C^1_{N_c} + (N_c - 1)\, C^1_{N_t} + C^1_{N_{wd}}$, where $C^m_n = \frac{n!}{m!(n-m)!}$. Consequently, the total complexity of the JTIM-DCSK system is expressed as $\Upsilon_1 = (N_t + 1)\, N_c\theta + (N_{wd} + 2)\theta + C^1_{N_c} + (N_c - 1)\, C^1_{N_t} + C^1_{N_{wd}}$. For comparison purposes, the complexities of several advanced benchmark systems are also summarized in Table 2.

Fig. 4 presents a comparison of the complexity per transmitted bit among five different DCSK schemes, where m_{tot} denotes the total number of transmitted bits per symbol period. The comparison parameters for those systems are set as follows: 1)$N_c = 2$, $N_t = 2$, N_{wd}=2 for JTIM-DCSK; 2)$N_c = 2$, $N_t = 2$, N_{wd}=4 for MIM-DCSK; 3)$N_c = 3$ for HIM-MC-DCSK, 4)$N_c = 4$, $M = 4$, N_{wd}=2 for CIM-MC-MDCSK. Owing to the intrinsic characteristics of these DCSK systems, it is not feasible to set m_{tot} to an identical value across all systems. As illustrated in Fig. 4, the complexity of the proposed JTIM-DCSK system is slightly higher than that of the HIM-MC-DCSK system, while remaining lower than those of the CIM-MC-MDCSK and conventional DCSK systems. Furthermore, it is the same as the MIM-DCSK system.

4. Numerical results and discussions

The primary focus of this section is to present simulation results that demonstrate the BER performance of the proposed JTIM-DCSK system and compare it against several advanced counterparts, thereby highlighting the advantages of the proposed system. Unless otherwise specified, β represents the spreading factor and ξ denotes the data rate in the following simulation

Table 1. Data rate comparison among the JTIM-DCSK system and other advanced counterparts

System	Data Rate
JTIM-DCSK	$\frac{N_c N_t+\log_2 N_c+(N_c-1)\log_2 N_t+\log_2 N_{wd}}{\beta T_c}$
MIM-DCSK	$\frac{N_t[\log_2 N_c+(N_c-1)\log_2 N_t+(N_c-1)\log_2 N_{wd}+(N_c-1)(N_t-1)]}{(N_t+1)\beta T_c}$
HIM-MC-DCSK	$2N_c/(\beta T_c)$
CIM-MC-MDCSK	$(\log_2 N_{wd} + N_c \log_2 M)/(\beta T_c)$
DCSK	$1/(\beta T_c)$

Table 2. Complexity comparison among the JTIM-DCSK system and other advanced counterparts

System	Complexity
JTIM-DCSK	$(N_t+1)\,N_c\theta + (N_{wd}+2)\theta + C^1_{N_c} + (N_c-1)\,C^1_{N_t} + C^1_{N_{wd}}$
MIM-DCSK	$(N_c-1)N_t\theta + \theta + (N_c-1)N_{wd}\theta + (N_c-1)(C^1_{N_{wd}} + C^1_{N_t}) + C^1_{N_c}$
HIM-MC-DCSK	$(3+N_c)\theta + N_c C^1_2$
CIM-MC-MDCSK	$(2N_c + N_{wd}N_c)\,\theta + C^1_{N_{wd}}$
DCSK	2θ

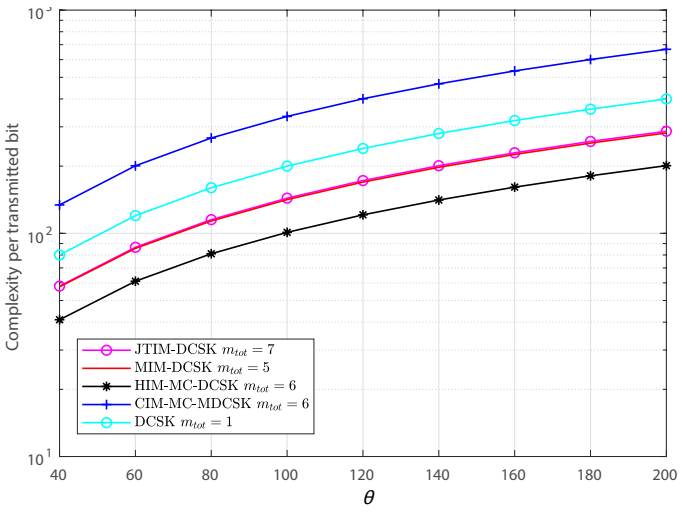

Figure 4. Complexities per transmitted bit of the JTIM-DCSK system and other advanced counterparts with various paramete θ

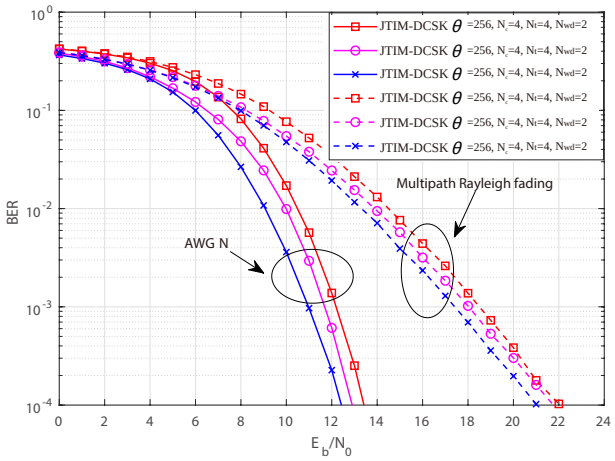

Figure 5. Simulated BER results of the JTIM-DCSK system for various values of N_t and N_c under two common channel model conditions

results. For the multipath Rayleigh fading channel, the parameters are configured as follows: the number of paths is set to $L = 3$; each path exhibits an identical average power gain (i.e., $E\left[\lambda_1^2\right] = E\left[\lambda_2^2\right] = E\left[\lambda_3^2\right] = 1/3$); the path delay $\tau_1 = 0$, $\tau_2 = 1$, $\tau_3 = 2$.

The impact of parameters N_c and N_t on the BER performance of the JTIM-DCSK system in both AWGN and multipath Rayleigh fading channels is illustrated in Fig. 5. The results indicate that the BER performance of the JTIM-DCSK system improves as the number of subcarriers and time slots increases. For example, when the number of subcarriers N_c increases from 4 to 8, the JTIM-DCSK system achieves a 1 dB gain at a BER of 10^{-4} over an AWGN channel.

Fig. 6 illustrates the simulated BER performance of the proposed JTIM-DCSK system under two common channel model conditions. For example, when we fix all the parameters except the spreading factor β, we can see that the BER performance of the JTIM-DCSK system decreases as the spreading factor increases from 256 to 500, suggesting that lower spreading factors

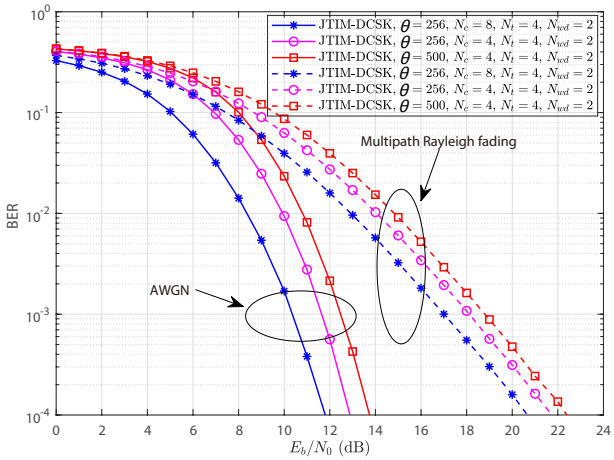

Figure 6. Simulated BER results of the JTIM-DCSK system for various values of θ and N_c under two common channel model conditions

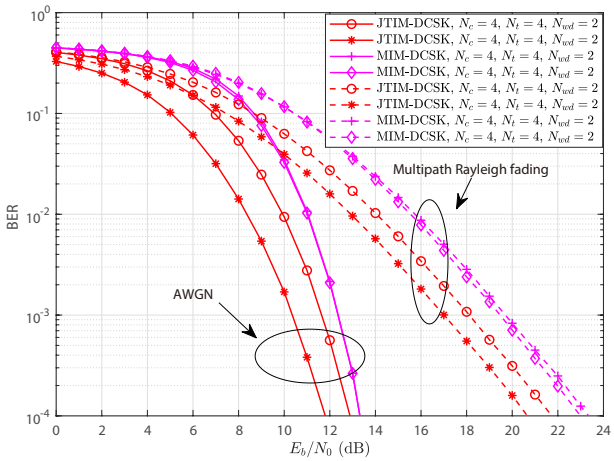

Figure 7. Comparison of BER results of the JTIM-DCSK and MIM-DCSK systems with $\theta = 256$ under two common channel model conditions

lead to better BER performance. This is mainly because as the spreading factor increases, the variance of the decision variable with respect to the noise also increases further, which makes the negative effect of the noise more significant.

The BER performance comparison between the proposed JTIM-DCSK system and the MIM-DCSK system is shown in Fig. 7. These results indicate that the BER performance of the proposed JTIM-DCSK system is notably superior to that of the MIM-DCSK system under two common channel model conditions. For example, when $N_c = 8$, $N_t = 4$ and $N_{wd} = 2$, the proposed JTIM-DCSK system is able to obtain a performance improvement of about 2 dB compared with the MIM-DCSK system at a BER of 10^{-4} . It is also evident that as the number of subcarriers enhances from 4 to 8, the BER performance of the proposed JTIM-DCSK system is further improved and the increase is

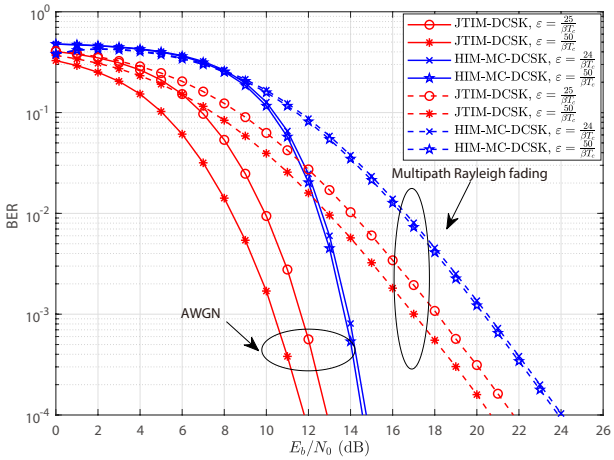

Figure 8. Comparison of BER results of the JTIM-DCSK and HIM-MC-DCSK systems with $\theta = 256$ under two common channel model conditions

larger than that of the MIM-DCSK system. Because the number of reference chaotic signals increases as the number of subcarriers becomes larger, which leads to a further increase in the advantages offered by the noise reduction module.

The comparison of the BER performance between the JTIM-DCSK system and the HIM-MC-DCSK system is shown in Fig. 8. The proposed JTIM-DCSK system is simulated using the following parameters: $\xi = 25/(\beta T_c)$ $(N_c = 4,\ N_t = 4,\ N_{wd} = 2)$, and $\xi = 50/(\beta T_c)$ $(N_c = 8,\ N_t = 4,\ N_{wd} = 2)$, respectively. Additionally, the HIM-MC-DCSK system is simulated using the following parameters: $\xi = 24/(\beta T_c)$ (i.e., $N_c = 12$), and $\xi = 50/(\beta T_c)$ (i.e., $N_c = 25$), respectively. It is evident that the BER performance of the proposed JTIM-DCSK system outperforms that of the HIM-MC-DCSK system under both channel models. For example, when $\xi = 50/(\beta T_c)$, the JTIM-DCSK system can achieve a performance gain of 3.5 dB over the HIM-MC-DCSK system at a BER of 10^{-4} .

5. Conclusion

Driven by the rapid growth of data-intensive wireless applications, there is an increasing need for transmission schemes capable of delivering higher throughput while maintaining efficient waveform utilization. Against this backdrop, this paper develops a differential chaos shift keying framework integrated with three-dimensional index modulation, aiming to enhance transmission capability through a redesigned multidimensional signaling structure. In this scheme, indexing operations are jointly carried out over three separate domains so that extra information bits can be conveyed via coordinated resource selection, forming a more compact and flexible waveform architecture. By introducing the Hilbert transform into the

system design, those time slots and subcarriers that would otherwise remain idle are converted into effective carriers of modulated symbols, which significantly improves time–frequency resource exploitation. Analytical complexity evaluation shows that the proposed JTIM-DCSK scheme requires fewer computational operations than both the CIM-MC-MDCSK and the conventional DCSK schemes. Furthermore, performance comparisons in terms of bit error rate and achievable data rate demonstrate clear advantages over existing advanced approaches. In particular, under two representative channel models, the proposed scheme attains an approximate 2–3.5 dB gain relative to competing systems while simultaneously providing higher transmission rates. By combining efficient multidimensional resource mapping, the inherent confidentiality properties of chaotic signals, and strong adaptability to time-varying channel conditions, the proposed JTIM-DCSK scheme offers a compelling solution for secure and high-efficiency waveform design in future dynamic wireless communication environments.

Funding

This work was supported by the Guangzhou College of Technology and Business Quality Engineering Project (YLZY202301, KCJYS202404); Foshan City Self-Financial Scientific and Technological Innovation Projects (2520001003014).

Availability of Data and Material

The data sets used and analyzed during the current study are available from the corresponding authors on a reasonable request.

Acknowledgements

This work was preprinted at https://www.researchsquare.com/article/rs-5173688/v1. It has not been peer reviewed by a journal.

Conflict of Interest

The authors declare that they have no potential conflict of interest with respect to the research, authorship, and publication of this article.

References

[1] T. Huang, J. Chen, H. Zeng, G. Cai, and G. Kaddoum, "Dual-Domain Deep Learning-Assisted NOMA-CSK Systems for Secure and Efficient Vehicular Communications," *IEEE Transactions on Communications*, vol. 74, pp. 7,480–7,493, Apr. 2026, doi: 10.1109/TCOMM.2026.3683818.

[2] C. Peng, Y. Tan, D. Ma, Z. Yang, C. Zhang, and Y. Fang, "A Novel Design of Low-PAPR OFDM-DCSK Waveform With Riemann Matrix-Based G-SLM for ISAC," *IEEE Communications Letters*, vol. 30, pp. 1,533–1,537, Mar. 2026, doi: 10.1109/LCOMM.2026.3676299.

[3] C. Duan, Y. Tao, Y. Fang, G. Han, and M. Guizani, "Multi-Carrier DCSK Scheme With Matrix Index Technique: A New Transmission Scheme for Physical Layer Security," *IEEE Journal on Selected Areas in Communications*, vol. 44, pp. 3,798–3,811, Mar. 2026, doi: 10.1109/JSAC.2026.3669883.

[4] Q. Lai, D. Huang, X. Chen, and X. Sun, "Design and Analysis of Parameter-Controlled Multiscroll Memristive Chaotic System With Application to Secure Communication," *IEEE Internet of Things Journal*, vol. 13, no. 10, pp. 21,720–21,729, Feb. 2026, doi: 10.1109/JIOT.2026.3666806.

[5] G. Zhang, K. Zhang, Y. Hu, and X. Jia, "Hybrid Time-Slot Selection-Carrier and Reference Index Modulated Differential Chaos Shift Keying System," *IEEE Transactions on Communications*, vol. 74, pp. 3,532–3,546, Jan. 2026, doi: 10.1109/TCOMM.2026.3653852.

[6] Y. Fang, Y. Pan, H. Ma, D. Ma and M. Guizani, "A Novel DCSK-Based Linear Frequency Modulation Waveform Design for Joint Radar and Communication Systems," *IEEE Transactions on Green Communications and Networking*, vol. 9, no. 1, pp. 354-366, Mar. 2025, doi: 10.1109/TGCN.2024.3422262.

[7] Z. Li, Y. Yang, D. Yan, and Y. Wang, "An Adaptive Combining Hybrid FSO/RF Terrestrial-Satellite Links Communication System Based on DCSK," *IEEE Photonics Technology Letters*, vol. 38, no. 15, pp. 1,058–1,061, Jan. 2026, doi: 10.1109/LPT.2026.3651509.

[8] L. He, Y. Xue, and X. Wu, "Multiple Time Slot Index and Code Index Applied to DCSK Systems - More Full Utilization of Time Slot Index," *IEEE Wireless Communications Letters*, vol. 15, pp. 1,115–1,119, Dec. 2025, doi: 10.1109/LWC.2025.3649565.

[9] L. He, Y. Pei, G. Zhang, and Y. Guo, "A Modulated Position-Indexed Differential Chaos Shift Keying System With Enhanced BER and Throughput," *IEEE Communications Letters*, vol. 30, pp. 612–616, Dec. 2025, doi: 10.1109/LCOMM.2025.3646108.

[10] G. Zhang, X. Wu, and Y. Xue, "Enhancing Multi-Carrier Chaotic Communication: Integrating Hybrid Code Sort and Chaotic Reference Index Modulation in DCSK System," *IEEE Transactions on Vehicular Technology*, vol. 75, no. 6, pp. 10,554–10,568, Jun. 2026, doi: 10.1109/TVT.2025.3643130.

[11] W. K. Xu, L. WANG, and G. Kolumbán, "A new data rate adaption communications scheme for code-shifted differential chaos shift keying modulation," *International Journal of Bifurcation and Chaos*, vol. 22, no. 08, p.1250201, Aug. 2012, doi: 10.1142/S021812741250201X.

[12] Z. Li, P. Chen, G. Chen, and Y. Fang, "Code index modulated chaotic ambient backscatter communication with differential walsh codes," *IEEE Wireless Communications Letters*, vol. 13, no. 4, pp. 999–1003, Apr. 2024, doi: 10.1109/LWC.2024.3355503.

[13] H. Yang and G.-P. Jiang, "High-efficiency differential-chaos-shift-keying scheme for chaos-based noncoherent communication," *IEEE Transactions on Circuits and Systems II: Express Briefs*, vol. 59, no. 5, pp. 312–316, May. 2012, doi: 10.1109/TCSII.2012.2190859.

[14] G. Kaddoum, E. Soujeri, and Y. Nijsure, "Design of a short reference noncoherent chaos-based communication systems," *IEEE Transactions on Communications*, vol. 64, no. 2, pp. 680–689, Feb. 2016, doi: 10.1109/TCOMM.2015.2514089.

[15] G. Kaddoum, F.-D. Richardson, and F. Gagnon, "Design and analysis of a multi-carrier differential chaos shift keying communication system," *IEEE Transactions on Communications*, vol. 61, no. 8, pp. 3281–3291, Aug. 2013, doi: 10.1109/TCOMM.2013.071013.130225.

[16] Y. Tao, Y. Fang, P. Chen, H. Ma, and M. Guizani, "Matrix reconstruction algorithm-assisted multi-carrier DCSK scheme: An effective solution for frequency-selective fading channe," *IEEE Wireless Communication Letters*, vol. 12, no. 11, pp. 1941–1945, Nov. 2023, doi: 10.1109/LWC.2023.3300353.

[17] H. Yang, G.-P. Jiang, W. K. S. Tang, G. Chen, and Y.-C. Lai, "Multi-carrier differential chaos shift keying system with subcarriers allocation for noise reduction," *IEEE Trans. Circuits Syst. II-Express Briefs*, vol. 65, no. 11, pp. 1733–1737, Nov. 2018, doi: 10.1109/TCSII.2017.2752754.

[18] B. Chen, L. Zhang, and Z. Wu, "General iterative receiver design for enhanced reliability in multi-carrier differential chaos shift keying systems," *IEEE Transactions on Communications*, vol. 67, no. 11, pp. 7824–7839, Nov. 2019, doi: 10.1109/TCOMM.2019.2939799.

[19] P. Chen, L. Wang, and G. Chen, "DDCSK-walsh coding: A reliable chaotic modulation-based transmission technique," *IEEE Transactions on Circuits and Systems II: Express Briefs*, vol. 59, no. 2, pp. 128–132, Feb. 2012, doi: 10.1109/TCSII.2011.2180109.

[20] X. Cai, W. Xu, S. Hong, and L. Wang, "A trinal-code shifted differential chaos shift keying system," *IEEE Communications Letters*, vol. 25, no. 3, pp. 1000–1004, Mar. 2021, doi: 10.1109/LCOMM.2020.3041460.

[21] G. Zhang, X. Chen, Y. Hu and Z. Luo, "Hybrid Carrier-Code and Reference Index Modulation in DCSK System With Time-Frequency Resources," *IEEE Transactions on Vehicular Technology*, vol. 74, no. 3, pp. 4148–4162, Mar. 2025, doi: 10.1109/TVT.2024.3485792.

[22] Y. Fang, D. Peng, H. Ma, G. Han, and Y. Li, "A neural network-aided detection scheme for index-modulation DCSK system," *IEEE Transactions on Vehicular Technology*, vol. 73, no. 2, pp. 2109–2121, Feb. 2024, doi: 10.1109/TVT.2023.3313813.

[23] X. Dou, T. Lyu, T. Han, and D. Liang, "A time-delay overlapping modulation based high spectral efficiency multi-user differential chaos shift keying for maritime internet of vessels," *IEEE Wireless Communications Letters*, vol. 13, no. 11, pp. 3227–3231, Nov. 2024, doi: 10.1109/LWC.2024.3460590.

[24] X. Cai, W. Xu, L. Wang, and G. Chen, "Towards high-data-rate noncoherent chaotic communication: A multiple-mode differential chaos shift keying system," *IEEE Transactions on Wireless Communications*, vol. 20, no. 8, pp. 4888–4901, Aug. 2021, doi: 10.1109/TWC.2021.3062836.

[25] Y. Fang, J. Zhuo, H. Ma, S. Mumtaz, and Y. Li, "Design and analysis of a new index-modulation-aided DCSK system with frequency-and-time resources," *IEEE Transactions on Vehicular Technology*, vol. 72, no. 6, pp. 7411–7425, Jun. 2023, doi: 10.1109/TVT.2023.3238379.

[26] H. Ma, Y. Fang, P. Chen, S. Mumtaz, and Y. Li, "A novel differential chaos shift keying scheme with multidimensional index modulation," *IEEE Transactions on Wireless Communications*, vol. 22, no. 1, pp. 237–256, Jan. 2023, doi: 10.1109/TWC.2022.3192347.

[27] G. Zhang, X. Wu, Y. Yang, and S. Shao, "Design and analysis of high data rate four-dimensional index modulation for differential chaos shift keying system," *IEEE Transactions on Wireless Communications*, vol. 23, no. 9, pp. 12 455–12 468, Sep. 2024, doi: 10.1109/TWC.2024.3392630.

[28] H. Ma, Y. Tao, Y. Fang, P. Chen, and Y. Li, "Multi-carrier initial-condition-index-aided DCSK scheme: An efficient solution for multipath fading channel," *IEEE Transactions on Vehicular Technology*, vol. 74, no. 10, pp. 15743-15757, Oct. 2025, doi: 10.1109/TVT.2025.3567450.

[29] Y. Tao, Y. Fang, H. Ma, S. Mumtaz, and M. Guizani, "Multi-carrier DCSK with hybrid index modulation: A new perspective on frequency-index-aided chaotic communication," *IEEE Transactions on Communications*, vol. 70, no. 6, pp. 3760–3773, Jun. 2022, doi: 10.1109/TCOMM.2022.3169214.

[30] Fadhil S. Hasan, "Design and analysis of grouping five-dimensional index modulation for high data rate DCSK communication system," *Digital Signal Processing*, vol. 163, pp. 105211, Aug. 2025, doi: 10.1016/j.dsp.2025.105211.

[31] G. Cai, Y. Fang, J. Wen, S. Mumtaz, Y. Song and V. Frascolla, "Multi-Carrier M-ary DCSK System With Code Index Modulation: An Efficient Solution for Chaotic Communications," *IEEE Journal of Selected Topics in Signal Processing*, vol. 13, no. 6, pp. 1375-1386, Oct. 2019, doi: 10.1109/JSTSP.2019.2913944.